11 WCEE

Paper No. 2152. (quote when citing this article)
Eleventh World Conference on Earthquake Engineering
ISBN: 0 08 042822 3

NONLINEAR DYNAMIC BEHAVIOR OF THE GROUND INFERRED FROM STRONG MOTION ARRAY RECORDS AT KOBE PORT ISLAND DURING THE 1995 HYOGO-KEN NANBU EARTHQUAKE.

E. YANAGISAWA* and M. KAZAMA**

* Professor, **Associate Professor

Department of Civil Engineering, Faculty of Engineering, Tohoku University
Aramaki, Aoba, Aoba-ku, 980 Sendai

ABSTRACT

During the 1995 earthquake, the vertical array observation system installed by Kobe City, recorded accelerations over 0.5g. Using the records observed by the system, the authors have estimated average stress-strain relationships in the ground at Kobe Port Island. The stress was directly evaluated from earthquake acceleration records. The strain was evaluated from the relative displacement divided by the distance between adjacent observation points. The hysteretic deformation properties were analyzed from the following points of view: (1) Softening of the ground stiffness during the earthquake, (2) Liquefaction process of the reclaimed ground during the main shock, and (3) Nonlinear properties during the main shock and the aftershocks.

KEYWORDS

Array observation; Dynamic shear strain; Dynamic shear stress; Hyogoken nanbu earthquake; Softening; Liquefaction; Nonlinear behavior; Stress strain relation; Strong motion records;

INTRODUCTION

On January 17 in 1995, the Hyogo-ken Nanbu Earthquake, well known as "The Great Hanshin-Awaji Earthquake," attacked the Kansai district of Japan. The man-made Port Island in Kobe city had subsided by several tens of cm, and the harbor facilities at the island suffered severe damage. While studying the damage to this artificially filled island, it is very important to know how much force acted the ground and how the ground responded during the earthquake. Fortunately, the strong motion observation system installed by Kobe city government successfully recorded the main shock and a series of aftershocks. Many engineers and researchers analyze these historic records from various points of view for years to come.

The first research interest in the field of soil dynamics is to examine the nonlinear behavior of the ground subjected to significant strong motion. A number of earthquake response analyses using the strong motion records from Port Island have been already performed by many researchers (Ansary *et al.*, 1995, Nagase *et al.*, 1995, Taguchi *et al.*, 1995, Igarashi *et al.*, 1995, Cubrinovski *et al.*, 1995, Yoshida *et al.*, 1995, Ejiri *et al.*, 1995). The dynamic properties of ground were also determined by Kokusho et al. (Kokusho *et al.*, 1995) and Yoshida et al. (Yoshida *et al.*, 1995). Kokusho et al. used an inversion technique to estimate S-wave velocity and damping ratio corresponding to the main shock as well as one small aftershock. They studied the effect of soil liquefaction and nonlinear soil properties on the peculiar seismic amplification mechanism at the site. On the other hand, Yoshida et al. used a back-analysis technique with the extended Kalman filter. They discovered the shear modulus of the lower layer of artificially placed fill become less than 1/100 of the initial shear modulus estimated by the down hole test method.

As it is well known that Port Island was covered with sand blows due to liquefaction, there is no doubt that even the reclaimed "Masado" liquefied during the earthquake. The second question is what level of shear

stress was applied to the reclaimed ground, and thirdly, how the liquefaction developed. Ishihara et al. (Ishihara *et al.*, 1995) concluded, from a simple analysis based on liquefaction strength curve, that the shear stress ratio acting on the reclaimed ground was 0.4 to 0.7 and that the first or second pulse caused liquefaction.

For studying the dynamic shear behavior of soils, laboratory element tests such as cyclic triaxial tests and resonant column tests have been used to obtain stress-strain relationships. Few attempts have been made to evaluate the stress-strain relationship directly under actual earthquake loading. In recent years, by increase of the numbers of sites of seismic array observation, it becomes possible to evaluate stress-strain time histories of soils from actual earthquake records. The first results applying the technique can be seen in research by Koga et al. (Koga *et al.*, 1990). They performed shaking table tests of embankment seismic stability and studied the dynamic behavior of liquefiable sandy soils. However, the first application of the technique to actual earthquake records was by Zeghal et al. (Zeghal *et al.*, 1994, Zeghal *et al.*, 1995). Their research showed cyclic mobility behavior of dense sand deposits during the 1987 earthquake at a site in the Imperial Wildlife Management area (Zeghal *et al.*, 1994). Furthermore, using records from the Lotung downhole array in Taiwan (Zeghal *et al.*, 1995), they compared the dynamic properties of soils evaluated from the earthquake records with those of laboratory tests. This author has also applied this technique to one dimensional centrifuge shaking table tests and studied dynamic behavior of sandy soils subjected to high frequency loading (Kazama *et al.*, 1995a, Kazama *et al.*, 1995c). The accuracy of the technique regarding with wave velocity, seismograph installation spacing, and the frequency contents has also examined by the author (Kazama *et al.*, 1996).

The purpose of this paper is to evaluate what level of stress acted on the ground and how the ground behaved during the Kobe earthquake. The method used in this study for evaluating the stress strain is the direct evaluation technique using the vertical array observation records described above. Preliminary reports on the Kobe earthquake applying this technique are already available (Kazama *et al.*, 1995b, Elgamal *et al.*, 1995). In this study, special attention was paid to the following three items: (1) Softening of the ground stiffness during the earthquake, (2) Liquefaction process of the reclaimed ground during the main shock, and (3) Nonlinear properties during the main shock and the aftershocks.

REVIEW OF THE STRONG MOTION ARRAY AT KOBE PORT ISLAND

Figure 1 shows the soil profile as well as the wave velocity structure obtained from PS logging at the observation site in Kobe Port Island. Four seismographs were installed from the ground surface (K.P.*+4.5m) to a depth of 83.5m (K.P.-79m). In the figure, the shear wave velocity identified by Kokusho et al. are also shown. The unit weight used in this study, as shown in Figure 1, was estimated by the authors. Sugito et al. estimated the orientation error of the Port Island borehole array records (Sugito *et al.*, 1995). According to their study, an error of about 22 degree in the NS-EW plane at -79m was found. Thus, in this study, we corrected the data orientation at -79m records using this value.

In order to study the strain dependency of the dynamic shear modulus, the main shock data as well as a series of aftershocks' data are used as shown in Table 1. It should be noted that excess pore water pressure might remain during aftershock-01 and aftershock-02 occurred 3 minutes after the main shock.

EVALUATION STRESS AND STRAIN HISTORIES

Evaluation of Stress

If the wave propagation can be assumed purely one dimensional in the z direction, the equation of wave propagation can be written in the form of equations (1).

$$\frac{\partial \tau_{xz}}{\partial z} = \rho \frac{\partial^2 u_x}{\partial t^2}, \qquad \frac{\partial \tau_{yz}}{\partial z} = \rho \frac{\partial^2 u_y}{\partial t^2}, \qquad \frac{\partial \sigma_z}{\partial z} = \rho \frac{\partial^2 u_z}{\partial t^2} \tag{1}$$

*) K.P. is an abbreviation for Kobe Pile, which is mean sea level at Kobe Port.

Integrating the equations (1) from surface to depth z with the stress free surface boundary condition, the stress at level z can be expressed by equations (2).

$$\tau_{NS}(z,t) = \int_0^z \rho(z)\alpha_{NS}(z,t)dz$$
$$\tau_{EW}(z,t) = \int_0^z \rho(z)\alpha_{EW}(z,t)dz \qquad (2)$$
$$\sigma_{UD}(z,t) = \int_0^z \rho(z)\alpha_{UD}(z,t)dz$$

where subscripts NS, EW and UD represent the direction of the acceleration component. Using the distribution of the acceleration $\alpha(z)$ and mass density $\rho(z)$, we can calculate the stress at any depth z. In this study, the distribution of acceleration can be approximately determined from array records using linear interpolation.

Evaluation of Strain

The average strain in the each layer can be calculated from the relative displacement between adjacent observation points divided by the thickness of the layer. Considering the observation system at Port Island, the ground at the site was devided into three layers, of which four seismographs were located on the top, and the displacement of each observation point was calculated by double integration of the acceleration records. Since the uniform deformation in each layer is assumed, we can not estimate the stress and strain due to the high frequency motion, in which the assumption of the linear interpolation is not valid. According to the accuracy of the technique examined by the authors (Kazama *et al.*, 1996), assumed that 10% approximation error is allowable, the highest frequency we can evaluate is 1.2Hz for horizontal components of the main shock, 1.5Hz for ones of aftershocks and 7Hz for vertical components of all cases. These values are obtained from the wave velocities investigated by Kokusho et al. as shown in Figure 1.

On the other hand, when wave propagation is one dimensional, it is theoretically derived that the stress and strain are in proportion to particle velocity. Accordingly,

$$\text{(stress)} \propto \text{(particle velocity)*(phase velocity)*(density)} \qquad (3)$$
$$\text{(strain)} \propto \text{(particle velocity)/(phase velocity)} \qquad .$$

Therefore, by comparing the particle velocity amplitudes before and after filtering, we can interpret whether the main portions of stress and strain are affected or not by high frequency filtering. In our cases it is found that the velocity amplitude decreases by less than 10% to 20% after the filtering. Consequently, the high frequency filter used in this study probably dose not affect so many values of the stress and strain.

The Stress and Shear Strain Evaluated from The Main Shock

Shear stress Figure 2 shows the shear stress time histories from +2m to -12m at every 2m of the NS component during main shock. The main portion of the shear stresses consists of two or three cycles of waves with a period of around 1 second. The stress generally increases with depth, while the stress ratio, which is the stress normalized by the effective vertical confining pressure, changes with the depth in the range of 0.15 to 0.45. If we consider the shear stress ratio of the reclaimed ground, its values are about 0.3 in both the NS and EW directions. The maximum shear stress ratio, obtained by the composition of the NS with the EW component in time domain, is about 0.4. Incidentally, the maximum resultant shear stress ratio obtained from the data without filtering was about 0.5. The maximum axial stress ratio obtained from UD component is 0.15 to 0.25.

Shear strain Figure 3 shows the time histories of the average shear strain evaluated. The maximum shear strains generated in the ground were 1-2% for the reclaimed layer (+4.5m to -12m), 0.6% for the alluvial clay layer (-12m to -28m), and 0.1-0.2% for the diluvial layer (-28m to -79m). Locus of the shear strain in horizontal plane is displayed in Figure 4. Apparently, the predominant direction of the shear strain is

consistent with that of acceleration records (Sugito *et al*, 1996).

Axial strain Axial strain ε_z was evaluated by the same way as the shear strain. However, the phase characteristics of the displacement time history at -12m obtained from double integration was irregular compared with the records at the other observation points. No matter how high the frequency was used in the low cut filter, the phase characteristics did not improve. Consequently, the UD component record at -12m was excluded from the analyses.

STRESS STRAIN RELATIONSHIP

Main Shock

Using the stress and the strain time histories evaluated in the previous section, stress-strain relationships during main shock are plotted for each layer as shown in Figure 5. The stresses are evaluated at the middle of each layer. A significant nonlinear behavior is seen during main shock in the first layer compared to the second and third layers. This behavior reflects evidence of liquefaction in the reclaimed ground. In these figures, a rectangular box covering the extent of the loops was added. If an average shear modulus during earthquake will be defined as the gradient of a diagonal line, its values are obtained as shown in Table 2. This table also shows the average S-wave velocities calculated from the density and the average shear modulus. The S-wave velocities obtained gave a slightly smaller value than those identified by Kokusho et al. shown in Figure 1. It is likely that assumption of one dimensional propagation in shear wave was the correct.

As is already written, nonlinear behavior of the reclaimed ground was significant during the main shock. Figure 6 shows the detailed variation of the stress-strain relationship in NS direction of the reclaimed ground. We numbered every half cycle starting from 3 seconds in stress time history. From about 3 seconds, the shear strain gradually becomes larger and larger, and at 4 half-cycle the shear strain suddenly increases to around 1%. Regarding the liquefaction process, it is inferred that the reclaimed ground reached complete liquefaction of around 5 to 7 seconds. After 7 seconds, the maximum shear stress corresponds to a residual strength post-liquefaction.

From Figure 6, the shear modulus and shear wave velocities can be calculated and the values show gradual reduction reflecting the liquefaction process. The shear modulus are consistent with the velocity identified by Kokusho et al. Concerning the damping ratio, there is difficulty in evaluating a damping ratio under random loading. In particular, few obvious loops were found in the stress-strain plots. Incidentally, the damping ratio evaluated from relatively obvious loops show the values about 20% to 35%.

Aftershocks

In order to study the strain dependent dynamic behavior of the ground, we have analyzed the records obtained from aftershocks as shown in Table 1. However, when we were proceeding with the analysis, we found the same irregularity in the records for the -12m NS component from "aftershock1". That is why we could not analyze behavior about NS component from "aftershock1". In addition, because the small acceleration brought a reduction of the accuracy in low frequency range, we have used a 0.5 to 1.5Hz band pass filter to analyze some records.

Figure 7 shows the variation of the stress strain relationship in the reclaimed ground during "aftershock01" (3 minutes after main shock) to "aftershock6" (about 1 month after) for the EW component. Eight figures in Figure 7 were plotted by the same scaling ratio between lateral and vertical axis. Apparently, the stress-strain relationships of "aftershock01" and "aftershock02" are different from others. Accordingly, the shear modulus of "aftershock01" and "aftershock02" are smaller than others. Conversely, the roundness of the loop, which represents damping characteristics, of "aftershock01" and "aftershock02" is larger than others. These behaviors can not be already seen in the stress-strain relationship of "aftershock1" (3 hours after main shock). It suggests that an excess pore water pressure due to liquefaction was still remaining after 3 minutes, and that the excess pore water pressure completely dissipated in 3 hours after main shock.

Using the results obtained so far, the graphs of shear modulus versus shear strain are plotted in Figure 8. For not only in reclaimed ground, but also the alluvial clay layer, it is likely that the shear modulus recovery in " aftershock01" and "aftershock02" is rather small compared to others. Furthermore, comparing the shear modulus of aftershocks 1 to 3 (occurring from January 17 to 19) with those of aftershocks 4 to 6 (occurring after February 2), the shear modulus recovery could be also found in this period. The lines plotted in Figure 8 were G-γ curves used in design work (Kitazawa *et al.*, 1981), where we regarded first layer as sandy material, second layer as a clay material, and third layer as an intermediate material between sand and clay. G_{max} was estimated from S-wave velocity obtained from PS logging. First of all, interestingly, the shear modulus of each layer during main shock has good agreement with G-γ curve used for design. Comparing the reduction ratio of the shear modulus during main shock to initial shear modulus for each layer, we find the reduction equal to the 4-6% for the first layer at G_1, about 30% for second layer and 45-50% for third layer. Next, the shear modulus during "aftershock-01" and " aftershock-02" are far from G-γ curve. Finally, the shear modulus during aftershocks 4 to 6 have good agreement with the design G-γ curve again.

This shows the nonlinear deformation characteristics of soils subjected to the significantly large earthquake motion in a real ground.

CONCLUSION

Nonlinear dynamic behaviors of the ground during the 1995 Hyogo-ken Nanbu Earthquake have been studied using vertical array records at Kobe Port Island. The results obtained from this study are as follows:

(1) The maximum shear stress ratio evaluated during main shock was about 0.4 in the reclaimed ground. The maximum average shear strain generated during main shock was 1-2% for reclaimed ground (+4.5m to 12m), 0.6% for alluvial clay layer (-12m to -28m) and 0.1-0.2% for diluvial layer (-28m to -79m).
(2) The shear modulus evaluated by direct evaluation technique using array records has good agreement with those by identification technique using earthquake response analysis.
(3) From the evaluation of the stress-strain relationship in the reclaimed sand, it is inferred that the reclaimed ground reached complete liquefaction 1 or 2 cycles after being subjected to relatively large stresses.
(4) We compared the dynamic behavior of the ground during main shock with those during a series of aftershocks. Significant large softening was found during aftershocks within 3 minutes following the main shock. However, this behavior can not be seen during the aftershocks occurring after 3 hours. Thus, it suggests that an excess pore water pressure due to liquefaction remained after 3 minutes, and that the excess pore water pressure dissipated within 3 hours of main shock. The shear modulus recoveries were also found during a series of aftershocks occurred from January 17 to February 2.

These results indicate the effectiveness of the application of the direct evaluation technique to actual earthquake records. This technique makes it possible to discuss nonlinear site response not only with peak ground acceleration, but with stress-strain levels. Fruitful results will be expected in the future using direct evaluation technique.

REFERENCE

Ansary, M.A., F. Yamazaki, T. Katayama and I. Towhata (1995). One dimensional response analysis by effective stress method at a liquified site during the Great Hanshin Earthquake, 1995. *Proc. of the 50th Ann. Conf. of the JSCE*, **I-614**, 1228-1229.

Ejiri, J. and Y. Goto (1995). Identification of incident wave at Port Island using vertical array records. *Proc. of the 50th Ann. Conf. of the JSCE*, **I-568**, 1136-1137 (in Japanese).

Elgamal, A-W., M. Zeghal and E. Parra (1995). Identification and modeling of earthquake ground response. *Proc. of IS-Tokyo '95/1st. Intern. Conf. on Earthquake Geotechnical Engrg.*, **Preprint** , 51-90.

Igarashi S. and D. Arbert (1995). Energy-based liquefaction prediction of Kobe Port Island and comparison with effective stress analysis. *Proc.of the 50th Ann. Conf. of the JSCE*, **III-267**, 534-535 (in Japanese).

Ishihara K., S. Yasuda and K. Harada (1995). Characteristics of soil properties and behavior of the ground. *J. of the JSCE*, **80**, 7, 50-53 (in Japanese).

Kazama, M., H. Toyota and T. Inatomi (1995a). Stress strain relationship in soils directly obtained from centrifuge shaking table tests. *Proc. of the Int. Workshop on Wind and Earthquake Engrg. for Offshore*

and Hyogo-ken Nanbu Earthquake. *Tsuchi-to-Kiso*, **43,** 9, 39-43 (in Japanese).

Kazama, M., H. Toyota and T. Inatomi (1995a). Stress strain relationship in soils directly obtained from centrifuge shaking table tests. *Proc. of the Int. Workshop on Wind and Earthquake Engrg. for Offshore and Coastal Facilities*, 129-143.

Kazama, M., E. Yanagisawa (1995b). Stress strain relationship of the ground evaluated from vertical array observation records at Kobe Port Island. *Proc. of the 23rd JSCE Earthquake Engrg. Symposium*, 185-188 (in Japanese).

Kazama, M., E. Yanagisawa, H. Toyota and I. Towhata (1995c). Stress strain relationship of sandy soils directly obtained from 1-D centrifuge shaking table tests. *Proc. of IS-Tokyo '95/1st. Intern. Conf. on Earthquake Geotechnical Engrg.*, **2**, 711-716.

Kazama, M., H. Toyota, I. Towhata and E. Yanagisawa (1996). Stress strain relationship of sandy soils obtained from centrifuge shaking table tests. *Proc.of JSCE*, to be appeared. (in Japanese).

Kitazawa, S., N. Higaki and S. Noda (1981). Estimation of the maximum ground accceleration in Okinawa prefecture and Amami lsland. *Note of the PHRI*, 396, 28p (in Japanese).

Koga, Y. and O. Matsuo (1990). Shaking table tests of embankments resting on liquefiable sandy ground. *SOILS AND FOUNDATIONS*, **30**, 4, 162-174.

Kokusho, T., K. Satoh and M. Matsumoto (1995). Nonlinear dynamic response of soil ground during 1995 Hyogo-ken Nanbu Earthquake. *Tsuchi-to-Kiso*, **43,** 9, 39-43 (in Japanese).

Nagase, H., S. Tsujino, R. Shishido, N. Yoshida and S. Yasuda (1995). A study on liquefaction at Port Island during the 1995 Hyogo-ken Nanbu Earthquake. *Proc.of the 50th Ann. Conf. of the JSCE*, **III-265**, 530-531 (in Japanese).

Sugito, S., K. Sekiguchi, A. Yashima, F. Oka, Y. Taguchi and Y. Kato (1996). Correction of orientation error of borehole strong motion array records obtained during the south hyogo earthquake of Jan. 17, 1995. *Proc. of JSCE, J. of structural mechanics and earthquake engineering*, to be appeared.

Taguchi, Y., A. Tateishi, F. Oka and A. Yashima (1995). Three dimensional liquefaction simulation on array observation records during the Hyogo-ken Nanbu Earthquake. *Proc.of the 50th Ann. Conf. of the JSCE*, **III-266**, 532-533 (in Japanese).

Yoshida N. (1995). Earthquakc response analysis at Port Island during the 1995 Hyogoken-nanbu Earthquake. *Tsuchi-to-Kiso*, **43**, 10, 49-54 (in Japanese).

Yoshida I. and T. Kurita (1995). Back analysis of dynamic soil properties of Port Island with the observation data. *Tsuchi-to-Kiso*, **43**, 9, 44-48 (in Japanese).

Zeghal, M. and A.-W. Elgamal (1994). Analysis of site liquefaction using earthquake records. *J. of Geotech. Engrg. Div., ASCE*, **120**, 6, 996-1017.

Zeghal, M., A.-W. Elgamal, H.T. Tang and J.C. Stepp (1995) Lotung downhole array. II: Evaluation of soil nonlinear properties. *J. of Geotech. Engrg. Div., ASCE*, **121**, 4, 363-377.

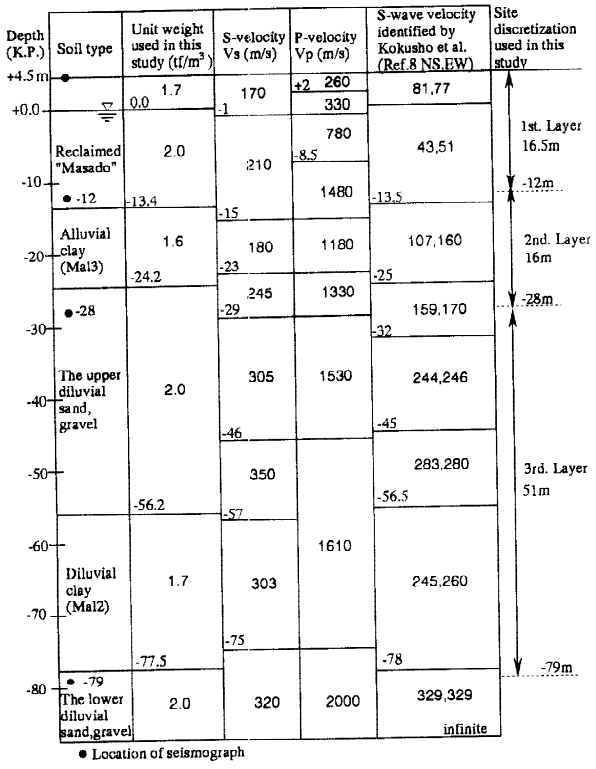

Fig.1 Soil profile of the observation site in the Kobe Port Island

Table 1 Events used in this study

Event	Occurrence time	Number of data	Used section (s)	Focal Depth (km)	Seismic Intensity in Kobe	M	Max. Acc. at surface *
Main shock	1995/1/17 5:46	36000	10-28	14	6	7.2	341
aftershock01	1995/1/17 5:49	36000	180-198	-	4	-	16
aftershock02	1995/1/17 5:49	36000	215-233	-	-	-	23
aftershock 1	1995/1/17 8:58	7000	7-25	18.8	4	4.7	46
aftershock 2	1995/1/18 5:25	12000	8-25	14.6	3	4.5	79
aftershock 3	1995/1/19 1:00	4600	6-24	13.6	2	4.0	13
aftershock 4	1995/2/2 16:04	4500	5-23	11.5	2	4.1	4
aftershock 5	1995/2/2 16:19	5500	8-24	17.9	3	4.2	65
aftershock 6	1995/2/18 21:37	5500	4-22	17.0	3	4.9	18

* show a larger value either NS or EW component

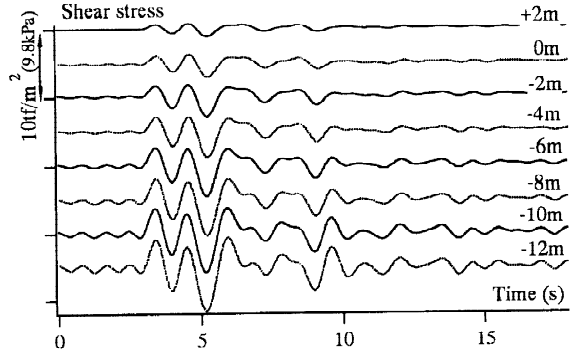

Fig.2 Time histories of shear stress for NS component of the main shock

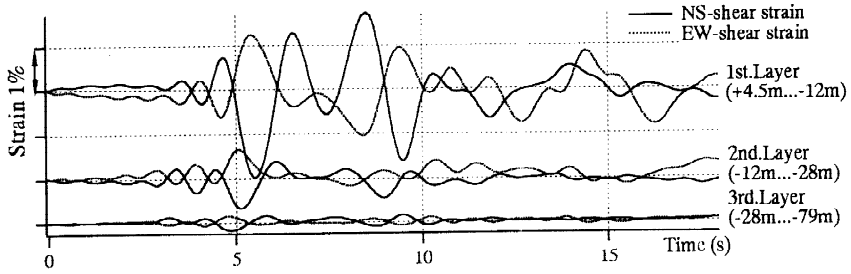

Fig.3 Time histories of average shear strain during the main shock

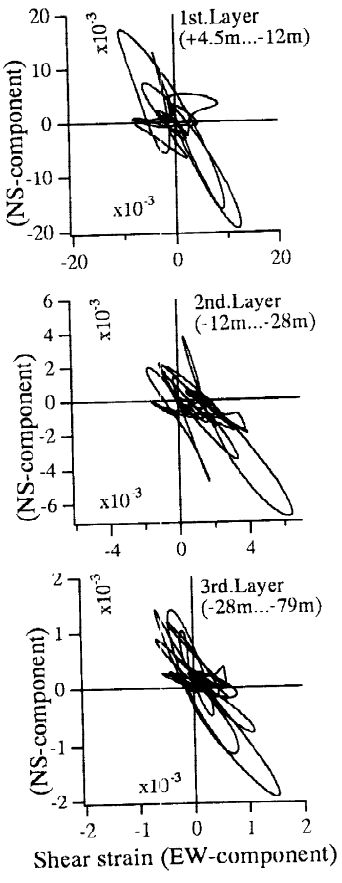

Fig.4 Shear strain loci in horizontal plane during the main shock

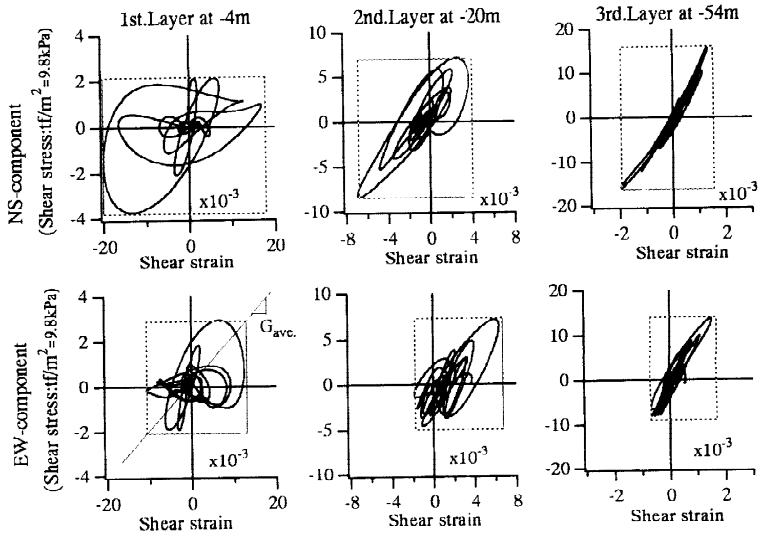

Fig.5 Stress-strain relationships during the main shock

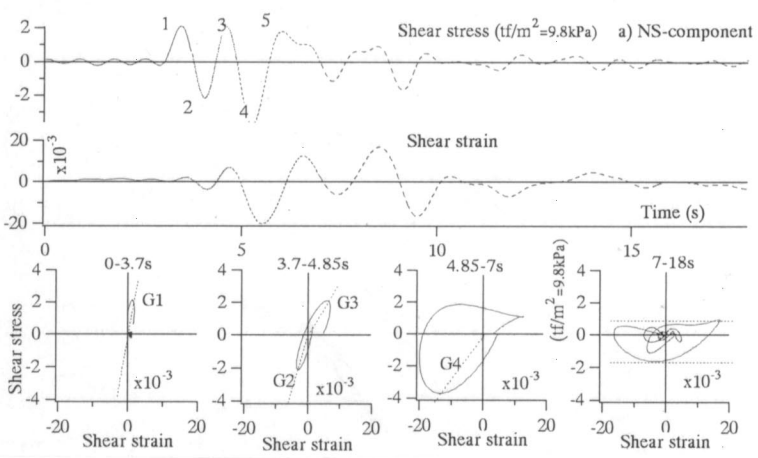

Fig.6 Stress-strain relationships of the reclaimed layer during the main shock

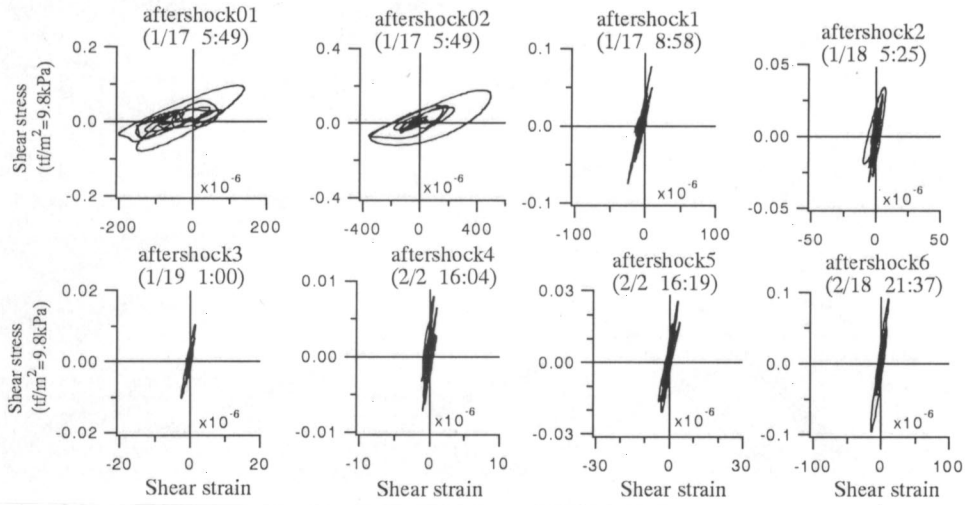

Fig.7 Change of stress-strain relationships of the reclaimed layer

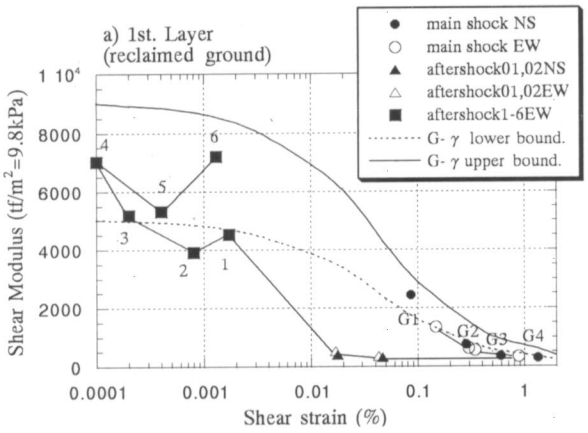

Table 2 Average shear modulus during the main shock

	layer No.	shear stress*	shear strain*	average shear modulus	density	average S-wave velocity
unit		(tf/m2)	%	Gave.(tf/m2)	(t/m3)	m/s
NS	1st.	2.93	1.850	158	1.90	29
	2nd.	7.71	0.532	1450	1.60	94
	3rd.	15.93	0.168	9510	1.85	224
EW	1st.	2.44	1.155	211	1.90	33
	2nd.	5.87	0.412	1425	1.60	93
	3rd.	11.06	0.111	9937	1.85	229

*show (maximum-minimum)/2 as an average value.

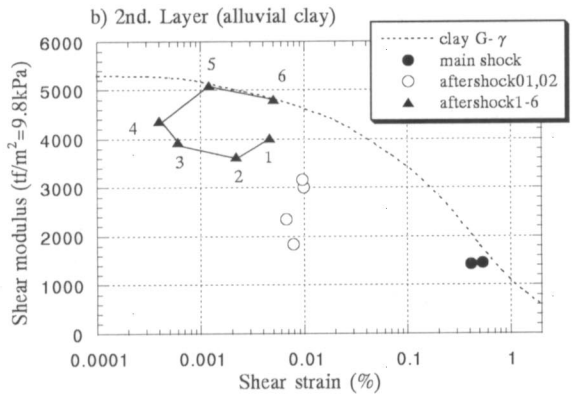

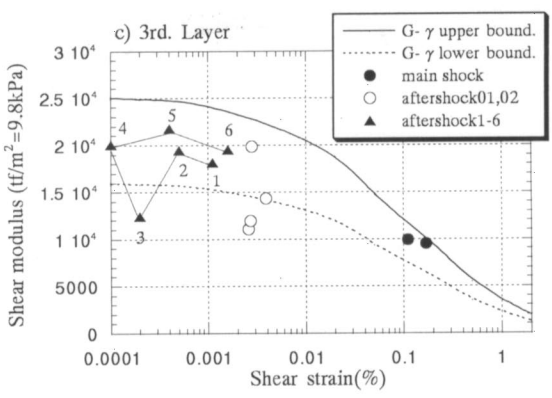

Fig.8 Variation of shear modulus with shear strain amplitude